applied sciences

MDPI

Article

The Characteristics of Deep-Water Gravity Flow in the Sublacustrine Fan of the Upper Triassic Yanchang Formation in the Huachi Area, Ordos Basin

Fengjie Li [1,2,3], Shuosi Chen [4,*] and Jia Wang [3]

[1] State Key Laboratory of Shale Oil and Gas Enrichment Mechanisms and Efficient Development, Beijing 102206, China; lifengjie72@163.com
[2] Sinopec Shale Oil and Gas Exploration and Development Laboratory, Beijing 102206, China
[3] Institute of Sedimentary Geology, Chengdu University of Technology, Chengdu 610059, China; wangjiacdut@163.com
[4] Exploration and Development Research Institute of Shengli Oilfield, China Petroleum & Chemical Corporation, Dongying 257015, China
* Correspondence: chenshs2026@163.com

Abstract

In the Ordos Basin, one of the most important oil- and gas-bearing basins, the Triassic Yanchang Formation has formed important source rocks, but is also a typical representative of continental deep-water sedimentation. In the Huacheng area of the Upper Triassic Yanchang Formation, the deep-water gravity flow sedimentation characteristics of the lake-bottom fan are complex, and the spatial distribution pattern and stacking style of the sand bodies are of great significance for oil and gas resource exploration. Based on core observation, by combining well logging and analysis of signs of sedimentary facies, including petrologic features and primary sedimentary structures, the thick massive sand bodies of the Chang 6 Member belong to deep-water gravity flow deposits, and they develop in a semi-deep to deep lacustrine environment in the Huachi area, Ordos Basin. The primary sedimentary structures of deep-water gravity flows include massive bedding, graded bedding, sliding fractures, slumping deformation structures, turbidite sequences, and synsedimentary offsets. Two kinds of deep-water gravity flows of the channel system, namely sandy debris flows and turbidity currents, were identified in the sublacustrine fan. The sublacustrine provided accommodation space for the rapid unloading and accumulation of gravity flows. Deposited sandy debris flows are the most widely distributed in the sublacustrine fan. Three types of stacked sand bodies developed in the Chang 6 Member of the Huachi area, including multi-stacked thick-layered, sandstone–mudstone interbedded, and sand-thin and mud-thick types. The multi-stacked thick-layered sand bodies consist of multi-period massive sandstones, which are interpreted as sandy debris flow deposits. Sandstone–mudstone interbedded types exhibit diverse lithologies, including massive sandstone and deformed structural sandstone. In addition, the turbidity current is the primary factor controlling the stacked sand bodies. Sand-thin and mud-thick sand bodies consist primarily of laminated mudstone, massive mudstone, and flaser-bedded sandstone, and these deposits were formed by waning-stage turbidity currents and the rigid heads of sandy debris flows.

Keywords: sublacustrine fan; sandy debris flows; turbidity current; depositional model; Upper Triassic; Ordos Basin

Check for updates

Academic Editors: Nikolaos Koukouzas and Nathan J. Moore

Received: 24 March 2026
Revised: 18 April 2026
Accepted: 22 April 2026
Published: 27 April 2026

Copyright: © 2026 by the authors. Licensee MDPI, Basel, Switzerland. This article is an open access article distributed under the terms and conditions of the Creative Commons Attribution (CC BY) license.

1. Introduction

Gravity flow deposits are widely developed in sedimentary basins all over the world, such as the Bay of Biscay, NE Atlantic [1], the fresh-water Lacustrine Rift Basin, the Paleogene Bach Long Vi Graben, Vietnam [2], the northern Bermuda Rise [3], and Ordos Basin in China [4]. Because it is an important sedimentary body for the occurrence of tight oil resources in sedimentary basins, it has attracted much attention from geologists.

The Triassic Yanchang Formation of the Ordos Basin has abundant tight oil resources developed in gravity flow deposits [4]. The Chang 6 Member (the sixth reservoir unit of the Triassic Yanchang Formation) in the Huachi area, located in the southwestern part of the Ordos Basin, is one of the tight oil enrichment layers in the gravity flow deposits [5–8]. The gravity flow deposits are characterized by thick massive sandstones, with the thickness of a single sand layer reaching about 0.6 to 1.5 m, and that of multi-layers reaching 10–20 m. As they are closely related to the accumulation of oil and gas, these sandstones have attracted widespread attention in recent years [9,10]. Over the years, scholars have held differing views on the causes of tight oil reservoir sand body formation in the Yanchang Formation, including thick massive turbidites [11,12]; slump turbidites [13]; slump turbidite fans or slump turbidite fans and slope shifting turbidite fans [14]; sandy debris flows [15–17]; or subaqueous sandy mass-transport deposits (SMTDs) [10]. These research results have enriched the theory of gravity flow deposits, but they have also brought significant difficulties to the analysis of the types of gravity flow deposits. Based on recent studies on the sedimentary characteristics of thick massive sandstone in the deep-water fan sedimentary system, geologists have suggested that thick massive sandstone that grew in the fan body primarily arose from sandy debris flow deposition [15,16,18–22]. The origin has gradually been accepted and applied in the sand body research of the Chang 6 Member. However, the evolution mechanisms of gravity flow deposits in the Chang 6 Member require thorough research.

In addition, the core samples from numerous drilling wells have revealed that two types of sand bodies including massive sand bodies and thin sand bodies are observed in the sublacustrine. There are various types of stacked patterns among these sand bodies. The stacked patterns of sand bodies effectively controlled the distribution and accumulation of oil, and had significant geological significance for oil in a deep-water sublacustrine. Therefore, this study makes full use of the core and well curve data from the Huachi area in the Ordos Basin to conduct a systematic study on the characteristics of different types of tight oil reservoir sand bodies in the Chang 6 Member", and deeply analyzes the stacking relationships of various tight oil reservoir sand bodies, and then establishes the formation models of tight oil reservoir sand bodies with multiple-event sedimentary causes under different sedimentary environments. This provides a reservoir prediction basis for the further exploration and development of tight oil in the Chang 6 Member in the Huachi area.

2. Geological Setting

The Ordos Basin is a large superimposed basin in northwestern China. Based on the basement and structural features, it is divided into six structural units. The Huachi area is located in the southwestern Yishan slope, in the central part of the Ordos Basin (Figure 1a).

During the Late Triassic Yanchang Formation sedimentary period, the Ordos Basin was a large-scale continental sag-type lake basin, and it exhibited the characteristic of continuous subsidence [5]. The Yanchang Formation is the primary oil-producing zone in the basin. Based on the oil content, the ten members are Chang 10 Member to Chang 1 Member in ascending order. A set of continental clastic rocks with a thickness of approximately 1200 m

was mainly deposited in the Yangchang Formation. The main types of sedimentary facies developed included rivers, alluvial fans and deltas [8].

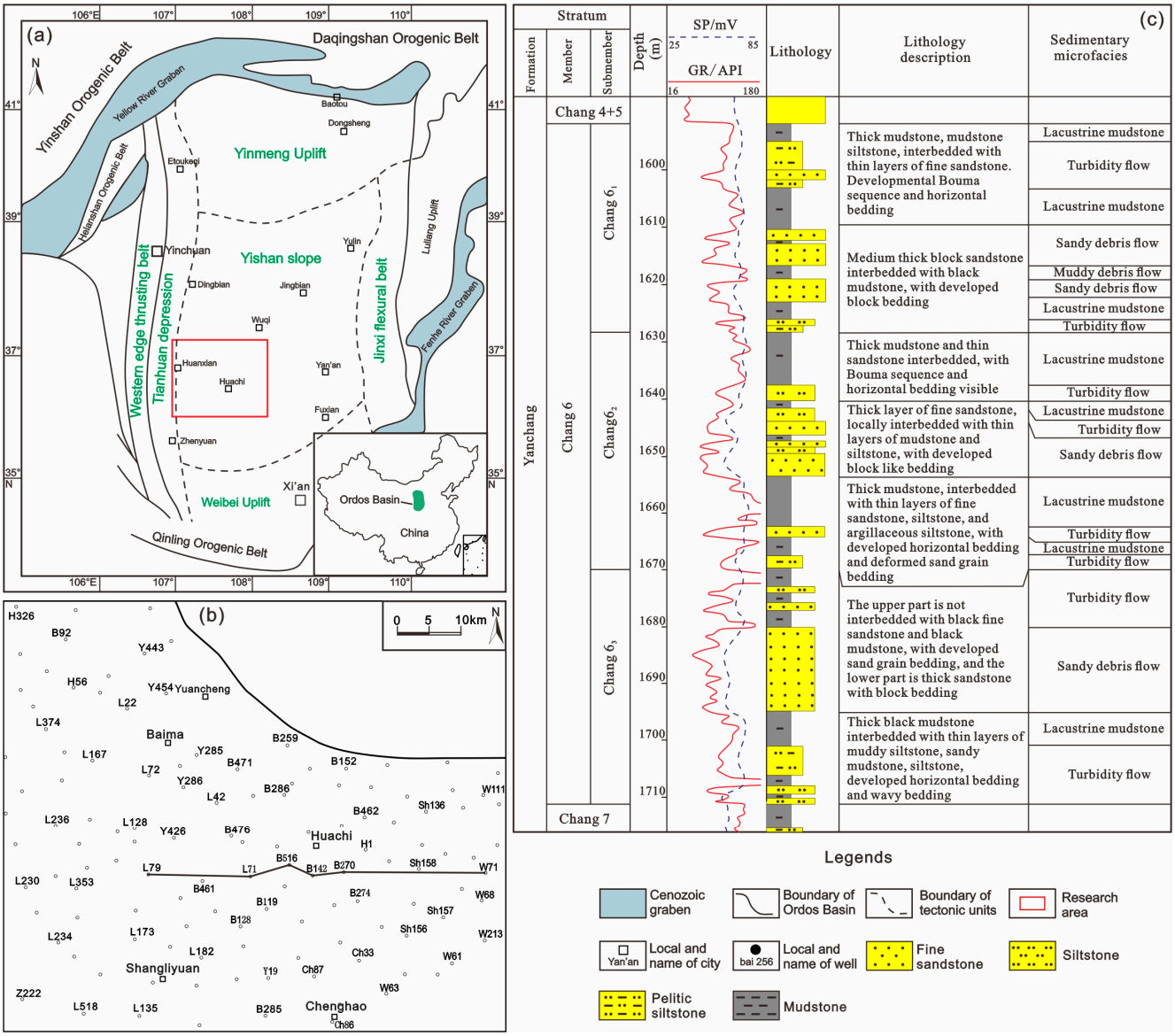


Figure 1. The tectonic division of Ordos Basin and location map of Huachi area (**a**). The main well location distribution in Huachi area (**b**); Tthe stratigraphic column of the Chang 6 Member, Ordos Basin (**c**) (modified from references [9,17]).

The Chang 6 Member was deposited during the retrogradational stage. Two deltaic sedimentary systems are distributed around the northeastern and southwestern parts of the lacustrine basin in the Huachi area [5]. The lithologies were characterized by thick blocky sandstone interbedded with thin layers of mudstone at the bottom of the Chang 6 Member. The middle and upper parts mainly showed interbedded deposition of dark gray mudstone and thin layers of fine to medium sandstone. Based on its lithological characteristics, the Chang 6 Member can be further divided into three submembers, namely Chang 6_1, Chang 6_2, and Chang 6_3 (Figure 1c). The sedimentary facies include sandy debris flow, turbidity current, and semi-deep lacustrine (Figure 1c).

3. Methods

A total of 15 cores was selected for sedimentary microfacies analysis on the basis of fine core observations of vertically variable data such as lithologic features and sedimentary structure. The core drilling wells are evenly distributed at different locations in the Huachi area to represent various depositional facies.

First, based on the observations of the drilling core, the sedimentary features, including of the lithology, sedimentary structure, and rock combination types, are described in detail. According to the features, the depositional facies of the Chang 6 Member are identified in the Huachi area.

Second, comparing the depositional facies identified from cores of drilling wells with the logging responses, various conversion models between the core facies and logging facies are established. Usually, the shape of the GR logging curve is used to interpret different types of sedimentary facies. The box shape or serrated box shape of GR logging curve corresponds with massive sand bodies, and the bell- or finger-shaped GR curves correspond to thin sand bodies. The average values of Gr curves in different types of GR curves shapes were referenced from previous studies [23–27].

Based on the established shape of the GR logging curve, 105 well logging curve data were analyzed to distinguish the types and the stacked pattern of sand bodies. At last, the distribution of facies was mapped across the Chang 6 Member in the Huachi area.

4. Results

4.1. Petrological Characteristics

The grain sizes of sandstone in the Chang 6 Member are primarily in the range of 0.15–0.2 mm, and the maximum is between 0.2 and 0.4 mm. The primary lithologies are lithic feldspar sandstone (Figure 2a) and feldspar lithic sandstone (Figure 2b). Occasionally, lithic sandstone (Figure 2c) can be found, which has poor grain sorting, with grains primarily being subangular.

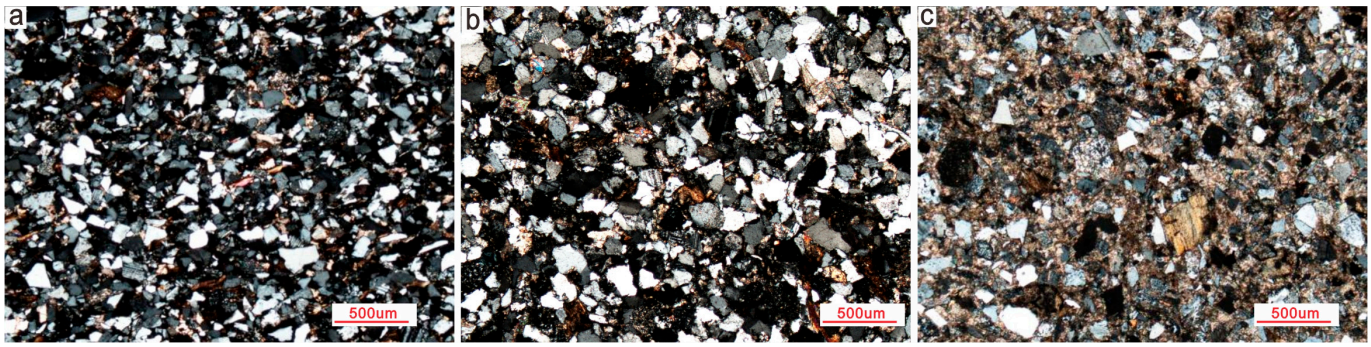


Figure 2. Characteristics of sandstone material components in the Chang 6 Member of the Huachi area. (**a**) Fine lithic arkose. Well Ch81, 1843.23 m, crossed polar. (**b**) Fine feldspathic lithic sandstone. Well W124, 2014.39 m, crossed polar. (**c**) Fine lithic sandstone. Well B221, 2057.2 m, crossed polar.

4.2. Sedimentary Structure Characteristics

Sedimentary structures of sandstones are abundant in the Chang 6 Member, and include massive bedding, graded bedding, slump deformation, and turbidite sequences.

Massive bedding of gray fine sandstone is the most common structure in the Chang 6 Member in the Huachi area (Figure 3a). Fragments of mudstone can on rare occasions be seen suspended and stretched in massive sandstone (Figure 3b), with a diameter of 2 to 6 cm. Massive bedding of fine sandstone is the typical sedimentary structure of sandy debris flow deposits [15,21].



Figure 3. The sedimentary structures of deep-water gravity flow in the Chang 6 Member of the Huachi area. (**a**) Gray fine sandstone with massive bedding; B488, 1863.9 m. (**b**) Gray fine sandstone with parallel bedding and massive bedding; normal graded bedding consisting of boulder-clay can also be seen. Well L170, 1944.63 m. (**c**) From bottom to top: gray-black mudstone with horizontal bedding, silty mudstone, siltstone with parallel bedding and inverse graded bedding. Well Ch80, 1967 m. (**d**) Gray fine sandstone, with normal graded bedding changing to inverse graded bedding in an upward direction. Well B 476, 2038.5 m. (**e**) Gray-white mudstone gradually changing to light gray fine sandstone with slump deformation structure, distal turbidite. Well Ch81, 1784 m. (**f**) From bottom to top: fine sandstone with graded bedding (yellow arrow line), silty mudstone, siltstone with parallel bedding, gray-black mudstone with horizontal bedding, inverse graded bedding. Well Ch80, 1990.4 m. (**g**) Gray-white siltstone with parallel bedding and gray horizontal bedding in mudstone. Well L125, 2040.1 m. (**h**) Light gray fine boulder feldspathic lithic sandstone with slump lenticular boulder-clay. Well Sh157, 1895.71 m. (**i**) Gray-white fine sandstone with slump lenticular clayey gravel. Well Ch80, 2003 m. (**j**) Gray-white lenticular sandy mudstone with small synsedimentary offset with the yellow dotted lines. Well Ch81, 1817.2 m. Sa, Sb, and Se, respectively, represent divisions a, b, and e of the Bouma Sequence.

Normal grading (Figure 3b), inverse grading (Figure 3c) and inverse–normal grading (Figure 3d) are also developed in local sandstones. The turbidity current depositions have rich associated sedimentary structures, including the Bouma Sequence, flame structure, and scour structure at the bottom [12]. The complete Bouma Sequence usually includes five divisions: Sa, Sb, Sc, Sd, and Se [28]. The Sa division represents high-density turbidity current deposits with massive or graded bedding; the Sb division exhibits parallel laminations of fine sandstone; the Sc division displays wavy or convolute laminations; the Sd division shows siltstone with horizontal laminations; and the Se division consists of dark mudstone with horizontal laminations. The Bouma Sequences are widely distributed in the Huachi area, but are often incomplete, commonly preserving only the lower divisions, such as Sa-Sb-Se (Figure 3e,f) and Sa-Se (Figure 3f,g).

Other sedimentary structures include sliding fractures (Figure 3h,i), slumping deformation (Figure 3g), and synsedimentary offset (Figure 3i).

4.3. Sedimentary Facies Analysis

4.3.1. Sedimentary Facies Types

According to previous studies on morphology [11,13–16,29,30], as well as on particle-supported mechanisms and deposition processes [31–35], the gravity flow deposition of the deep-water fan in the Chang 6 Member can be divided into two types: (a) the fluidized sediment flows of the non-channel system and (b) the sandy debris and turbidite flows of the channel system. As the fluidized sediment flows did not develop in the Huachi area, the primary focus of this study is on introducing the sedimentary characteristics of sandy debris flows and turbidity currents.

Sandy Debris Flow

According to its genetic mechanism [16,31–33,36], sandy debris flow is a kind of plastic fluid called Bingham fluid [31–33]. Depositions of sandy debris flow in the Chang 6 Member are very common in the Huachi area, including gray and brown massive medium–fine sandstone, usually in the middle of the gravity flow. In the coarser sandstone rhythmic bedding, floating tabular or torn syn-genetic boulder-clay is clearly visible, and it shows normal (Figure 3b), inverse (Figure 3c), and inverse–normal grading (Figure 3d). At the bottom of sand bodies, the surface abruptly comes into contact with mudstone in the semi-deep to deep lacustrine zone. The thickness of a single sand body is normally larger than 0.5 m, and the sand bodies change rapidly in the lateral direction. Sometimes they superpose from meters to tens of meters or even more than twenty meters. The matrix (illite) is the major interstitial material, and the average content is about 5–9%. Sandy debris flows have good physical reservoir properties and an obvious oil inrush (Figure 3a). All of these features make the sandstones from sandy debris flows favorable reservoirs in the local oil field. The bottom of the SP curve is an abrupt interface, reflecting an unconformity, and it may develop a scoured surface in a high-energy state. The GR curve in Figure 4 presents a large box consisting of multi-stacked boxes (Figure 4).

Turbidity Current

Gray and brown-gray thick-layered fine sandstone with black mudstone inside is deposited at the lower part of the turbidite sequence, and gray-black siltstone with argillaceous siltstone in deep-water mudstone commonly develops at the upper part. The Bouma Sequence is always fragmentary in cores, and the most common combination is an interbed of sandstones and shales, forming a cyclotherm with stable thickness. A single sand body ranges from centimeters to tens of centimeters, and the maximum is less than 0.5 m. According to the location and moving distance of the turbidity current, it can be divided into a proximal and a distal turbidity current.

The proximal turbidity current primarily consists of thin–medium fine sandstone, siltstone, and silt–mudstone. Scour structures at the bottom (Figure 3h), as well as flame structures, can be found, and only the Sa-Sb-Se and Sb-Se parts of the Bouma Sequence have been preserved (Figure 3h). The proximal turbidity current is widely distributed in front of the sandy debris flow, inside the transport channels, on both sides of the levees, and in the frontal lobe, while the distal turbidity current is at the forefront of the deep-water fan. With increasing moving distance, the turbidity current fluid keeps diluting and is finally deposited in the deep-water. The depositions primarily consist of deep gray siltstone with ripple bedding, gray-black sandy mudstone with horizontal bedding, and mudstone. From the bottom to the top, the lithology gradually transits to mudstone in deep lacustrine facies (Figure 3i). The Bouma Sequence here only retains the Sd-Se part, and on rare occasions, scour structures at the bottom and flame structures can be seen.

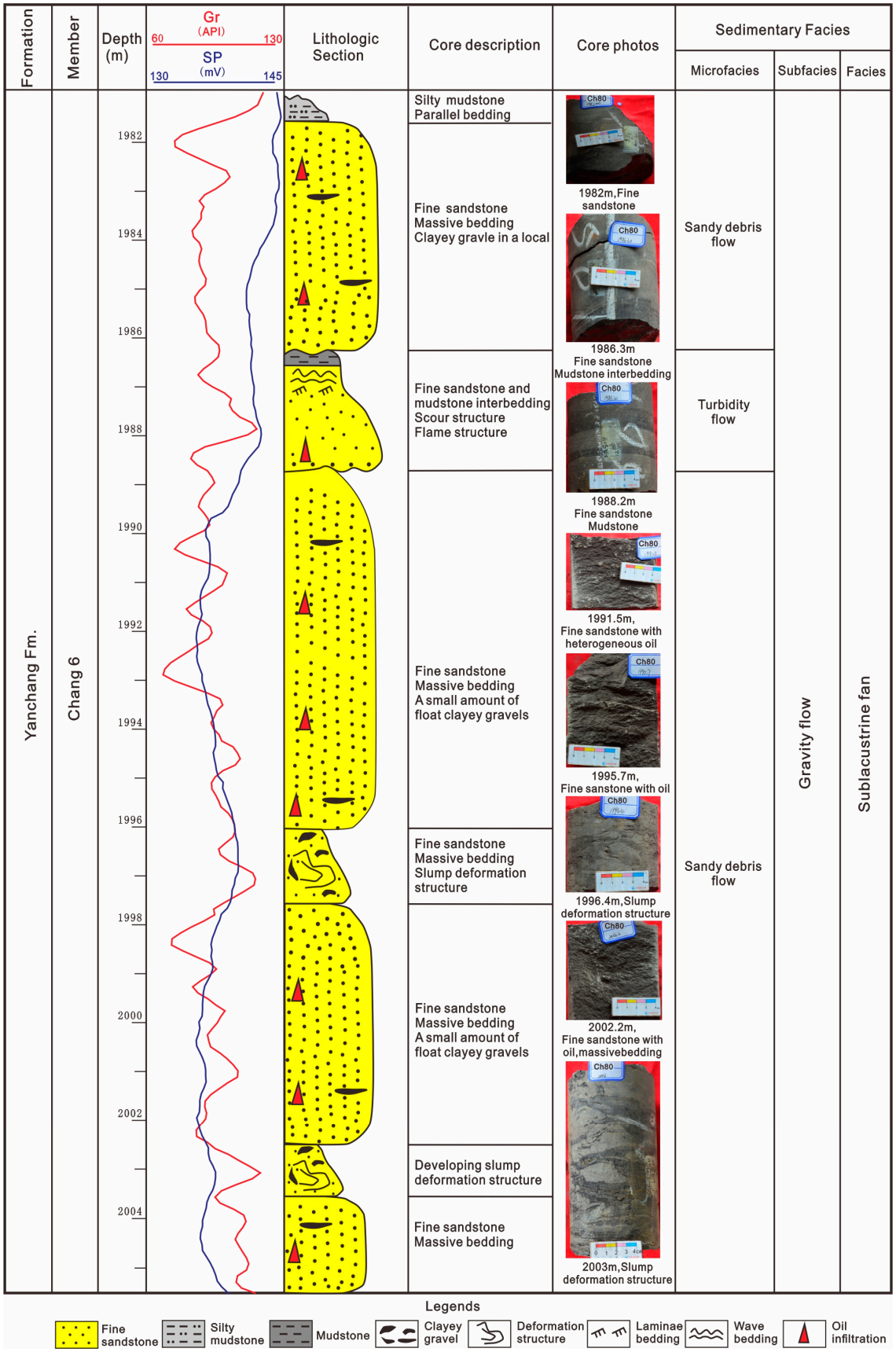


Figure 4. Common sedimentary assemblages of fluidized sediment flow, sandy debris flow, and turbidity current of the Chang 6 Member of Well Ch80 in the Huachi area, Ordos Basin.

According to the lateral comparison profile of the depositionally connected well (Figure 5), the local deposits are from the gravity flow in semi-deep lacustrine environments, especially the sandy debris flow in the Chang 6_3 and Chang 6_2 reservoirs. The Chang 6_1 reservoir lacks gravity flow deposition and consists of turbidites. Gravity flow extends along the south and north directions in the Huachi area, and the northern part is thicker than the southern part.

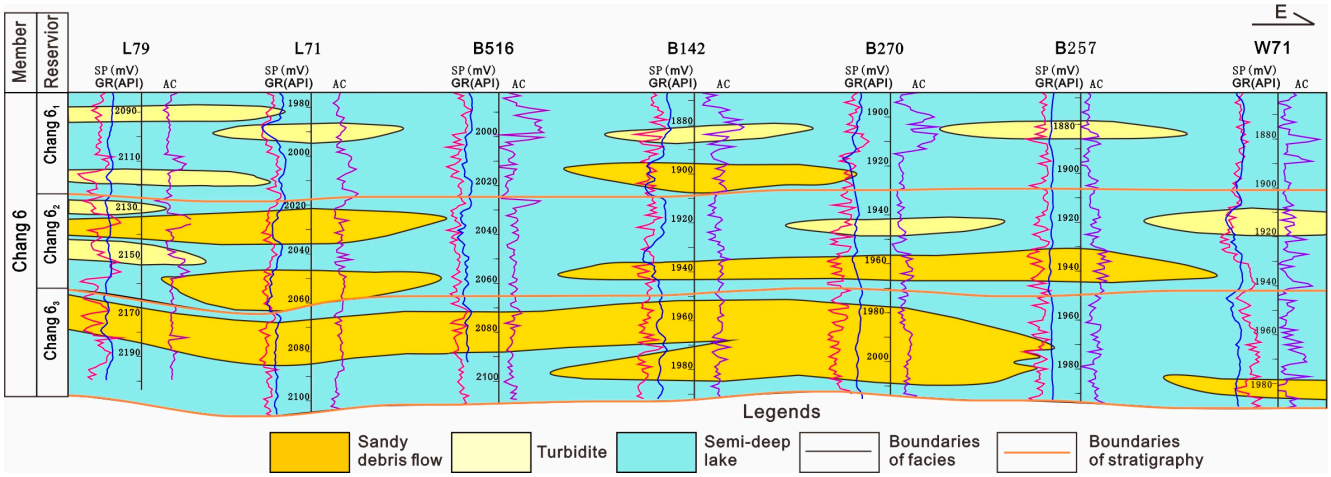


Figure 5. Lateral comparison profile of the sedimentary connected well of the Chang 6 Member in the Huachi area, Ordos Basin.

4.3.2. The Distribution of Sedimentary Microfacies

Based on the analysis of logging curve shape and the isopach map of the sand-to-stratum thickness ratio, a sedimentary microfacies distribution map of the Chang 6 Member in the Huachi area is presented in Figure 6. There was a semi-deep lacustrine environment developing in the Chang 6 Member, which the sublacustrine fan of gravity flow deposited in the Huachi area. It was distributed in a north-west to south-east direction, with the sandy clastic flow and turbidite flow particularly prominent in semi-deep lake sediment. The sedimentation of the sublacustrine fan was controlled by two source systems in the north-east and south-west directions. The turbidite deposits were developed in the middle of the Huachi area, while on both sides of this area are sandy debris flow deposits (Figure 6).

4.3.3. Gravity Flow Sedimentary Model

Based on the detailed analysis of the features of various gravity flows and their distributions, a sublacustrine fan model of the Chang 6 Member was established (Figure 7). During the deposition period of the Chang 6 Member, the lacustrine basin was in a contracting state. The surrounding deltas continuously accumulated in the basin, bringing in a large amount of terrestrial debris, which gathered in the Wuqi area. Periodic and sudden seismic events can cause the unstable front lobes at the delta front to collapse, resulting in the formation of liquefied sedimentary fluid sand bodies. The uppermost part of the liquefied sediment, under the influence of gravity, transforms into debris flows, which are further transported and form debris flow sedimentary sand bodies; the debris flow then advances further and transforms into turbidite sand bodies. With further seismic events, this process will repeat, causing different regions, sedimentary facies belts, and types of reservoir sand bodies to be superimposed vertically and closely coexist horizontally. In this way, the sediments will be strongly fluidized, slipping down the slope and becoming a gravity flow throughout the whole semi-deep lacustrine fan.

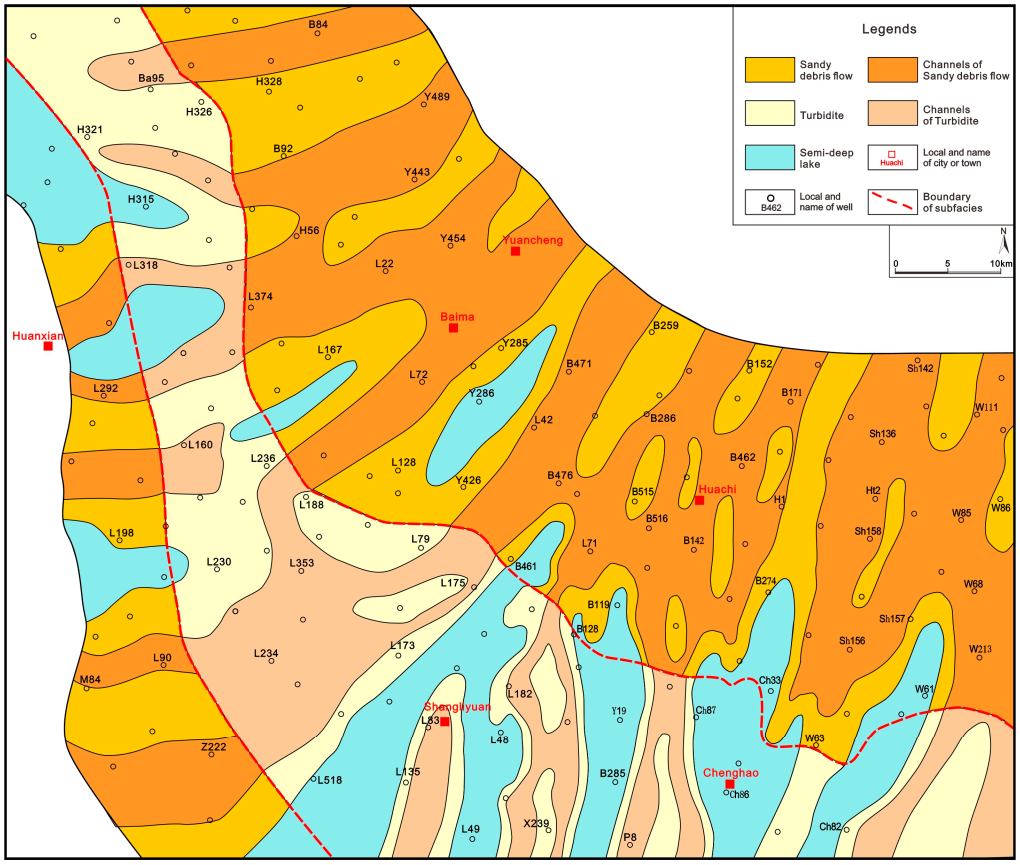


Figure 6. Sedimentary microfacies distribution of Chang 6 Member in Huachi area, Ordos Basin.

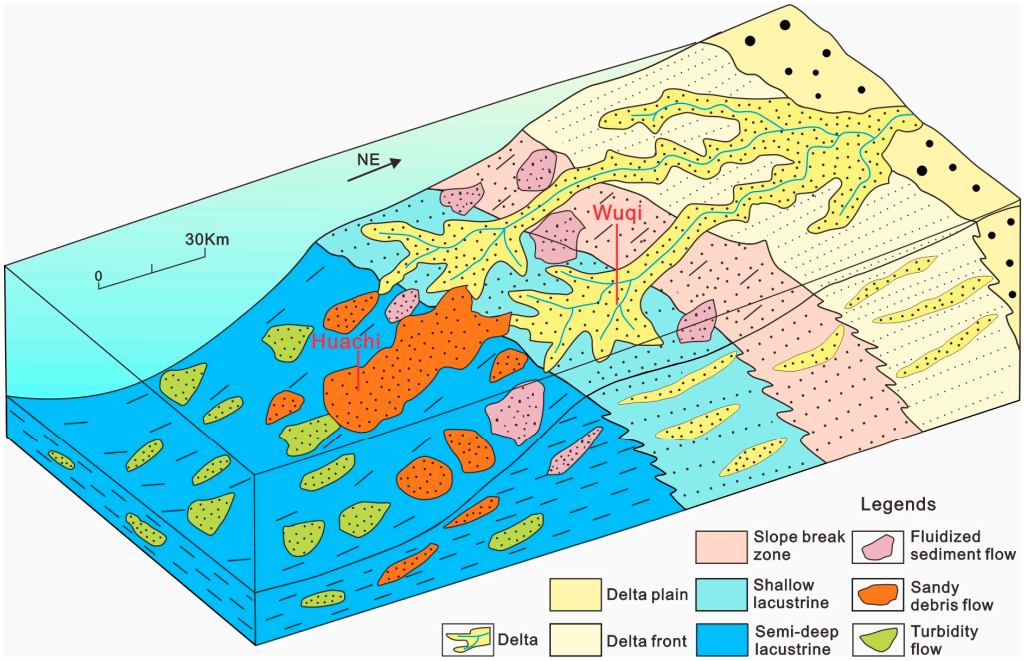


Figure 7. The sublacustrine fan "source and sink" model of the Chang 6 Member in the Huachi area, Ordos Basin.

5. Discussion

5.1. Type of Sand Body Stacking

Based on the interpretation of 105 well logging curve shapes, three sand body stacking types were developed in the Chang 6 Member of the Huachi area.

5.1.1. Massive Sandstone Stacking Type

The thickness of this type of sand body is generally more than 10 m with massive bedding. In the massive sand bodies (MS), multi-cycle erosion structures and clayey gravel sections can be observed (Figure 8a). These characteristics suggest episodic high-energy depositional pulses. Therefore, the stacked sand bodies developed sandstone with parallel laminated (PLS) and sandstone with flaser-bedding. The gamma-ray curve features exhibit a conspicuous box shape with a sand body thickness of 12 m (Figure 8b). Generally, the massive sandstone is interpreted as debris flow deposition and may indicate rapid sediment supply [7–10].

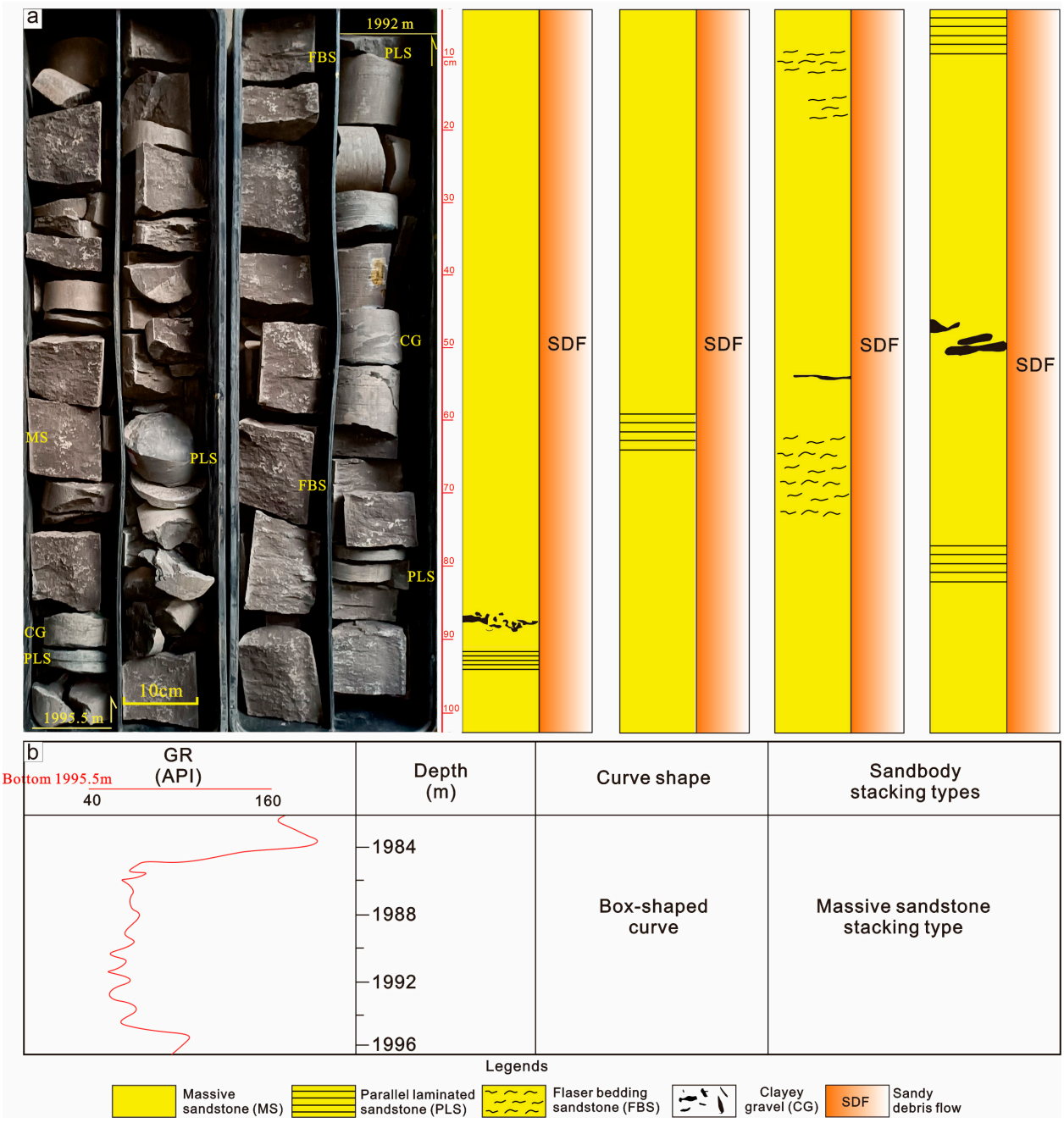


Figure 8. Analysis of core section and logging curve characteristics in Well B286. (**a**) Well B286, 1992–1995.5 m, the core of massive sandstone stacking type; (**b**) Well B286 GR, box-shaped curve feature.

5.1.2. Sandstone–Mudstone Interbedded Stacking Type

This type of sand body stacking consists of MS, PLS, and FBS; normal-grained sandstone (NGS); and deformable structural sandstone (DSS). The thickness of massive sandstone is relatively small, usually less than 15 cm, and accounts for a relatively small proportion of the sand–mud interbedded sand body. In contrast, although the thicknesses of PLS, FBS, and NGS are less than 10 cm, they occupy a relatively large proportion of the sand body. The mudstone, including massive mudstone (MM) and horizontal laminated mudstone (HLM), constitutes about 40–60% of the total section. The incomplete Bouma Sequence with Sa-Sb-Se or Sa-Se is observable (Figure 9a). In the stackings, rhythmic alternation reflects fluctuating energy conditions, which suggests cyclic events of turbidity current. The gamma curve predominantly exhibits a bell shape, a continuous serrated shape, and finger shapes (Figure 9b).

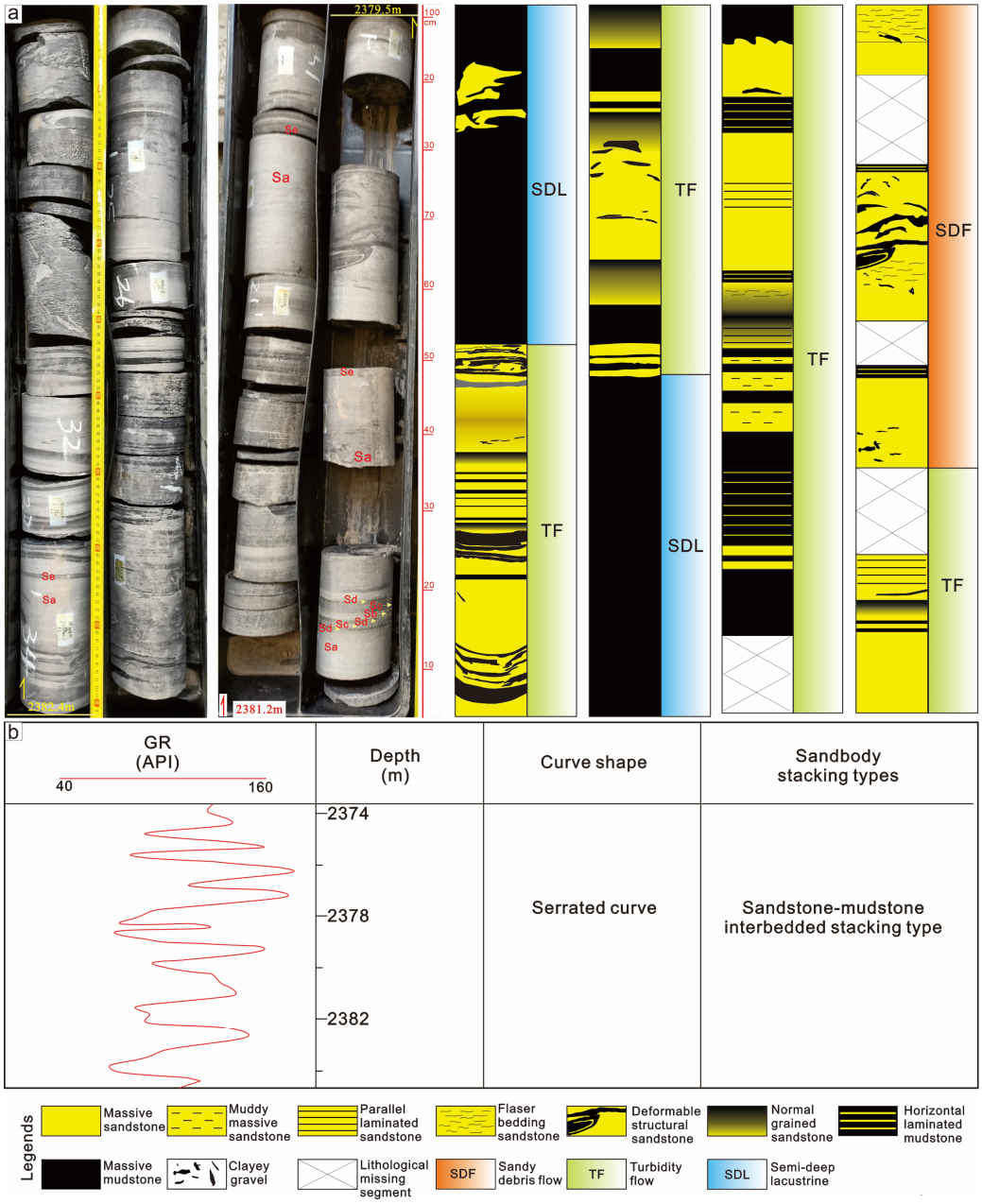


Figure 9. Analysis of core section and logging curve feature in Well H326. (**a**) Well H326, 2379.5–2382.4 m, the core of sandstone–mudstone interbedded stacking type; (**b**) Well H326 GR, serrated curve feature.

5.1.3. Sand-Thin and Mud-Thick Stacking Types

The thicknesses of sand bodies are less than 5 cm in the stacking; in contrast, the mudstones are thick, ranging from 25 cm to 50 cm, dominating the section with over 70% thickness (Figure 10a). The overall gamma curve is a combined finger shape, and the curve value is high (Figure 10b).

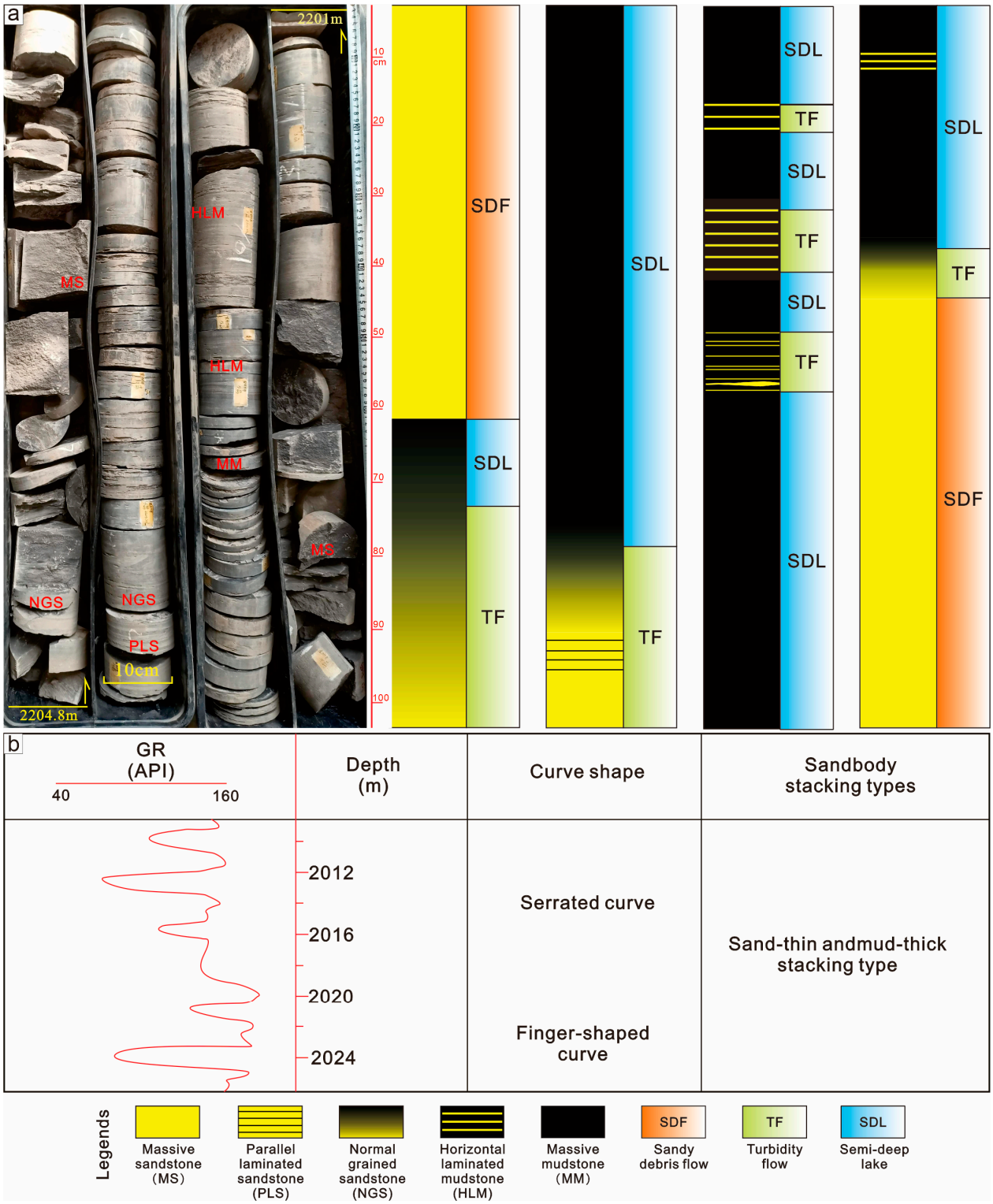


Figure 10. Analysis of core section and logging curve characteristics in L85. (**a**) Well L85 2201–2204.8 m, the core of sand-thin and mud-thick types; (**b**) Well L85 GR, finger-shaped curve feature.

5.2. The Process of Fluid Transport and Sedimentation

5.2.1. Liquefied Sediment Flow

The deposited sediments of the delta front, under the influence of triggering mechanisms such as earthquakes and volcanoes, first undergo fragmentation and sliding, and then gradual liquefaction, forming liquefied sediment flows. Li et al. (2018) referred to this as cohesive debris flow [10], and Tian et al. (2022) referred to it as seismite [9]. As the liquefied sediment flow moves downslope, it continuously tears the mudstone layer, causing the mudstone to break and form mudstone gravel, which is intermixed with the sandstone. At the same time, the mudstone layer undergoes sliding deformation, forming a sliding collapse structure (Figure 11a).

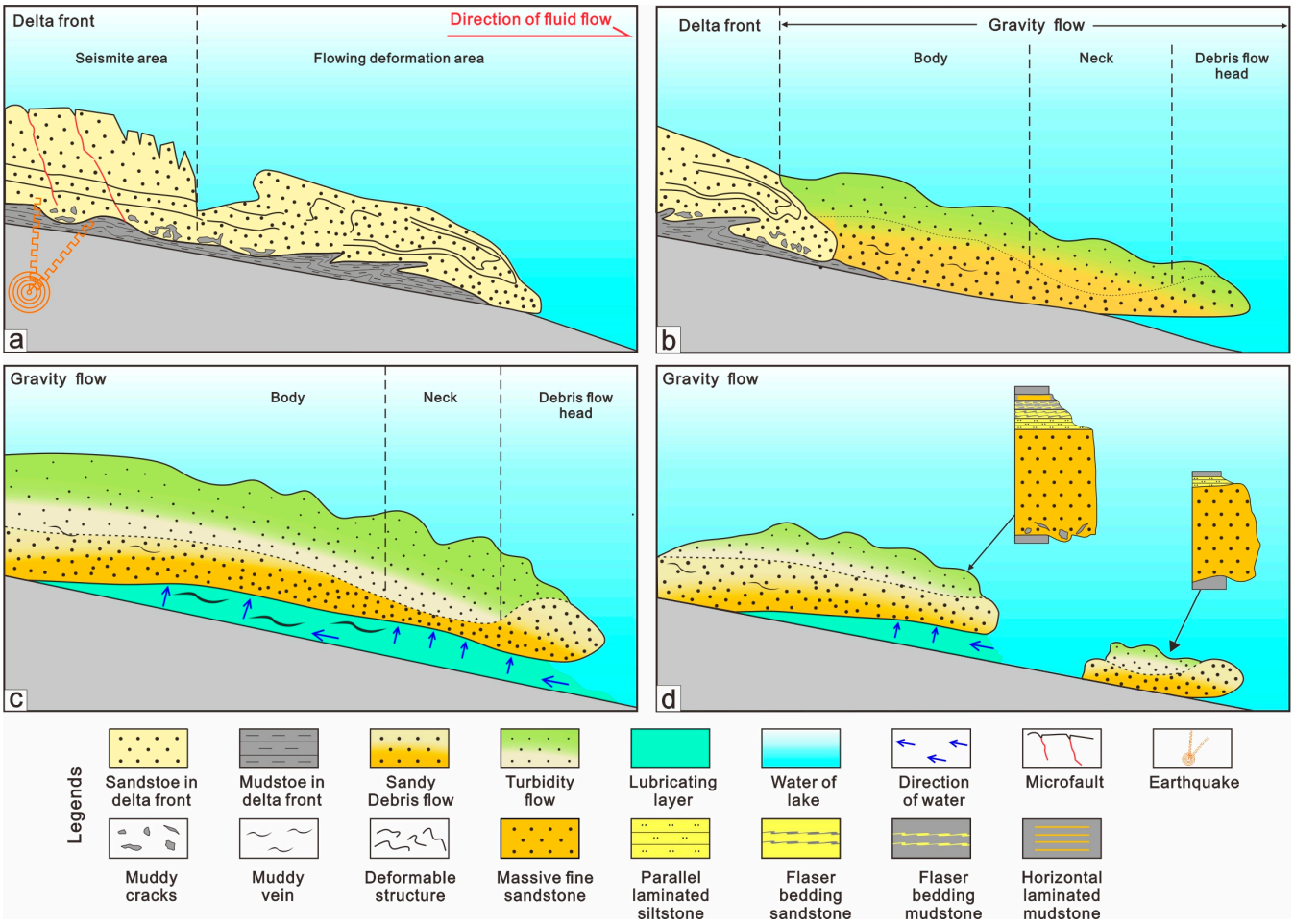


Figure 11. Transport process and deposit features of sandy debris flow (modified from reference [17]). (**a**) The deposited sediments of the delta front form liquefied sediment flows under the influence of triggering mechanisms. (**b**) The buoyancy causes the front part of the fluid to detach from the base, forming a head [37]. (**c**) The head and neck of the sandy debris flow are invaded by lubricating water layers; (**d**) the sandy debris flow separates from the head and continues to migrate under the influence of gravity.

5.2.2. Sandy Debris Flow

As the sediment continuous to liquefy, it produces sandy debris flows. In the course of transport and deposition, the clay content of sandy debris flows plays a critical role [37]. Under conditions of high clay content, buoyancy causes the front of the fluid to detach from the bottom, forming a head, and a water wedge is created between the head and the bottom of the sediment (Figure 11b). As the water flows down the slope, the range of

the water wedge gradually expands (Figure 11c). In the neck region, the head separates from the main body (Figure 11d). The front end of the separated main body then forms a new head, accompanied by a water wedge, thus initiating the second separation stage (Figure 11d). The separated head continues to move forward and eventually deposits in the semi-deep lake basin [38].

5.2.3. Turbidity Current

When the clay content is low, the viscosity of the fluid is low [37], and the main body of the fluid moves in a layered form. During the transportation process, the fluid will undergo erosion and decomposition, and the deposition speed is relatively fast. Therefore, the sediment is relatively uniform and consists of pure blocky sandstone. Their weak coherence leads to the preservation of thin, overlying, massive, and normal-grained sediments, corresponding to Bouma Sequence Sa, which represents high-density turbidity current deposits (Figure 12a).

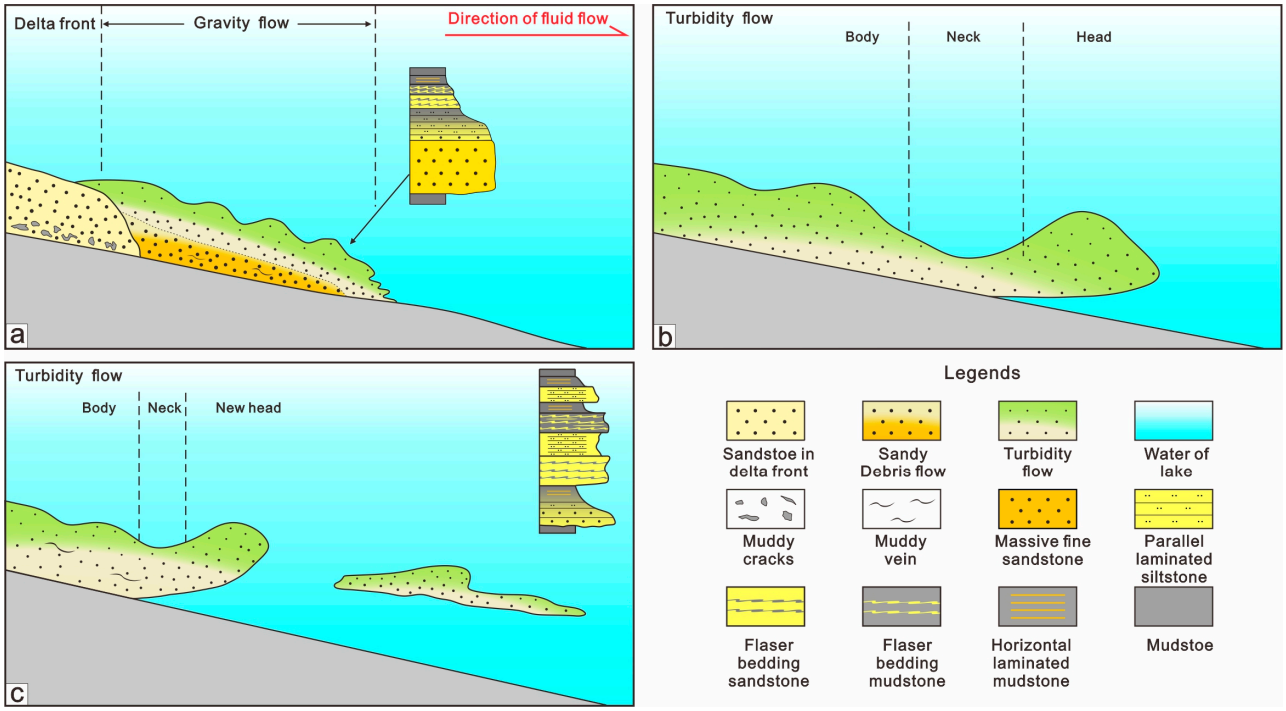


Figure 12. Transport process and deposit features of turbidity current (modified from reference [17]). (**a**) Transport process of sandy debris flow and continuous sedimentation, adapted from [37]. (**b**) Schematic diagram of the head of turbidity current rising and the neck forming during the transportation process of turbidity current. (**c**) The head of turbulent current separated from the body and the new head formation [38].

As the sediment continues to deposit, the fluid gradually evolves into a turbid flow. During sediment transportation along the slope, the turbidity current pushes the surrounding fluids backward, thereby increasing the velocity at the front part of the flow and forming a reverse circulation [17], and keeps the sediment suspended in the turbulent flow [38]. The front part of the turbidity current will be lifted by buoyancy (Figure 12b) and detach from the main body (Figure 12c).

5.3. Genetic Analysis of Stacked Sand Bodies

5.3.1. Massive Sandstone Stacking Type

During the flow process, the high-density sandy debris flow causes rapid accumulation of sand bodies, which are predominantly composed of massive sandstones with rare

occurrences of other current-induced sedimentary structures. In a short period of time, multiple layers of sandy debris flows were deposited one upon another, resulting in the formation of thick massive sand bodies.

5.3.2. Sandstone–Mudstone Interbedded Stacking Type

The interbedded sandstone–mudstone sequences with NGS, PLS, and HLM are primarily of turbiditic origin. These sedimentary assemblages represent sedimentary characteristics of turbidity currents. Due to the turbidity currents being low-density gravity flows, the thickness of the deposited sediment is relatively thin in each turbidity current event. After the turbidity current event, normal mudstone deposits were formed. In this way, repeated turbidity current events built up the interbedded sequence.

5.3.3. Sand-Thin and Mud-Thick Stacking Type

The sediments of the head separated from the turbidity current deposit in semi-deep and deep lacustrine settings and form isolated thin sandstones. This is because, in the deep lake, the turbidite sand bodies are rarely deposited, and most of the normal lake deposits are present. The HLM reflects the suspension clay deposit in the sustained deep lake.

6. Conclusions

(1) According to the analysis of petrological characteristics and primary sedimentary structures, in the thick massive sandstone of the Chang 6 Member in the Huachi area, Ordos Basin, two kinds of deep-water gravity flows of the channel system were identified in the sublacustrine fan: sandy debris flows and turbidity currents. A distribution model of gravity flow in the sublacustrine was established for the Chang 6 Member.

(2) Three types of stacked sand bodies, including massive sandstone stacking type, sandstone–mudstone interbedded stacking type, and sand-thin and mud-thick stacking types, developed in the Chang 6 Member of the Huachi area, Ordos Basin. The genetics of these stacked sand bodies are controlled by deposits, sandy debris flow and the turbidity current.

Author Contributions: Conceptualization, F.L.; methodology, F.L. and J.W.; investigation, F.L. and S.C.; writing—original draft preparation, F.L.; writing—review and editing, F.L., S.C., and J.W.; supervision, F.L.; project administration, F.L.; funding acquisition, F.L. All authors have read and agreed to the published version of the manuscript.

Funding: This research was funded by the Open Fund Project "Study on the Paleogeographic Evolution of Upper Permian and Shale Facies in the Northern Sichuan-Western Hubei Region" of the Sinopec Shale Oil and Gas Exploration and Development Laboratory [grant number 33550000-24-ZC0613-0023].

Institutional Review Board Statement: Not applicable.

Informed Consent Statement: Not applicable.

Data Availability Statement: The data is contained within the article.

Acknowledgments: We are grateful to the three anonymous reviewers for their valuable suggestions, which have significantly improved the quality of the paper.

Conflicts of Interest: Author Shuosi Chen was employed by the company Exploration and Development Research Institute of Shengli Oilfield, China Petroleum & Chemical Corporation. The remaining authors declare that the research was conducted in the absence of any commercial or financial relationships that could be construed as a potential conflict of interest.

References

1. Mulder, T.; SZaragosi, S.; Garlan, T.; Mavel, J.; Cremer, M.; Sottolichio, A.; Sénéchal, N.; Schmidt, S. Present Deep-Submarine Canyons Activity in the Bay of Biscay (NE Atlantic). *Mar. Geol.* **2012**, *295*, 113–127. [CrossRef]
2. Hovikoski, J.; Therkelsen, J.; Nielsen, L.H.; Bojesen-Koefoed, J.A.; Nytoft, H.P.; Petersen, H.I.; Abatzis, I.; Tuan, H.A.; Phuong, B.T.N.; Dao, C.V.; et al. Density-Flow Deposition in a Fresh-Water Lacustrine Rift Basin, Paleogene Bach Long Vi Graben, Vietnam. *J. Sediment. Res.* **2016**, *86*, 982–1007. [CrossRef]
3. Laine, E.P.; Hollister, C.D. Geological effects of the Gulf Stream system on the northern Bermuda Rise. *Mar. Geol.* **1981**, *39*, 277–310. [CrossRef]
4. Fu, J.H.; Dong, G.D.; Zhou, X.P.; Hui, X.; Dan, W.D.; Fan, L.Y.; Wang, Y.G.; Zhang, H.T.; Gu, Y.H.; Zhou, G.X. Research progress of petroleum geology and exploration technology in Ordos Basin. *China Petrol. Expl.* **2021**, *26*, 19–40.
5. Yang, H.; Liu, Z.L.; Zhu, X.M.; Deng, X.Q.; Zhang, Z.Y.; Qi, Y.L. Provenance and depositional systems of the Upper Triassic Yanchang Formation in the southwestern Ordos Basin, China. *Earth Sci. Front.* **2013**, *20*, 10–18.
6. Fu, S.T.; Yao, J.L.; Li, S.X.; Zhou, X.P.; Li, M.R. Enrichment characteristics and resource potential of continental shale oil in Mesozoic Yanchang Formation, Ordos Basin. *Petrol. Geol. Exper.* **2020**, *42*, 698–710.
7. Li, F.J.; Jiang, B.; Zhao, J.X. The sedimentary microfacies zoning and its genetic analysis of delta front in depressed-type lacustrine basin. *J. Mineral. Petrol.* **2008**, *28*, 111–117.
8. Zheng, R.C.; Wen, H.G.; Han, Y.L.; Wang, H.H.; Zheng, C.; Cai, J.L. Discovery and significance of sublacustrine slump turbidite fans in Chang 6 oil-bearing Formation of Baibao region in Ordos Basin, China. *J. Chengdu Univ. Technol.* **2006**, *33*, 566–575.
9. Tian, J.C.; Liang, Q.S.; Wang, F.; Yu, W. Genesis and development model of tight oil reservoir sand body in continental lacustrine basin: A case study on the Upper Triassic Chang 6 pay zone, Ordos Basin. *Oil Gas Geol.* **2022**, *43*, 877–888.
10. Li, X.B.; Liu, H.Q.; Pan, S.X.; Chen, Q.L.; WanYan, R.; Xu, W.L.; Wang, H.B.; Huang, J.P.; Wang, J. Subaqueous sandy mass-transport deposits in lacustrine facies of the Upper Triassic Yanchang Formation, Ordos Basin, Central China. *Mar. Petro. Geol.* **2018**, *97*, 66–77. [CrossRef]
11. Xia, Q.S.; Tian, J.C. Sedmientary characteristics of sublacustrine fan of the Interval 6 of Yanchang Formation of Upper Triassic in south western Ordos Basin. *J. Palaeogeogr.* **2007**, *9*, 33–43.
12. Stow, D.A.V.; Mayall, M. Deep-water sedimentary systems: New models for the 21st Century. *J. Mar. Pet. Geol.* **2000**, *17*, 125–135. [CrossRef]
13. Fu, Q.; Lv, M.M.; Liu, Y.D. Developmental characteristics of turbidite and its implication on petroleum geology in Late-Triassic Ordos Basin. *Acta Sediment. Sin.* **2008**, *26*, 186–192.
14. Chen, Q.H.; Li, W.H.; Guo, Y.Q.; Liang, J.W.; Cui, J.P.; Zhang, D.F. Turbidite systems and the significance of petroleum exploration of Yanchang Formation in the southern Ordos Basin. *Acta Geol. Sin.* **2006**, *80*, 656–663.
15. Li, X.B.; Liu, H.Q.; Wanyan, R.; Wei, L.H.; Liao, J.B.; Ma, Y.H. First discovery of the sandy debris flow from the Traissic Yanchang Formation, Ordos Basin. *Litho. Reserv.* **2001**, *21*, 20–21.
16. Li, X.B.; Chen, Q.L.; Liu, H.Q.; Wanyan, R.; Wei, L.H.; Liao, J.B.; Long, L.W. Features of sandy debris flows of the Yanchang Formation in the Ordos Basin and its oil and gas exploration significance. *Acta Geol. Sin.* **2001**, *85*, 1187–1202. [CrossRef]
17. Tang, W.W.; Tian, Y.M.; Li, F.J.; Zhao, J.X.; Zhao, K.L.; Wang, Z.Y. Genesis and Depositional Environments of Stacked Gravity-Flow Sandbodies in the Chang 6 Member, Maling–Qiaochuan Area, Ordos Basin, China. *Geol. J.* **2026**, *Online ahead of print*. [CrossRef]
18. Shanmugam, G. 50 years of the turbidite paradigm (1950s~1990s) deep-water process sand facies models—A critical perspective. *J. Mar. Pet. Geol.* **2000**, *17*, 285–342. [CrossRef]
19. Mutti, E.; Benoulli, D.; Ricci Lucchi, F.; Tinterri, R. Turbidite and turbidity currents from Alpine 'flysch' to the exploration of continental margins. *Sediment* **2009**, *56*, 267–318. [CrossRef]
20. Zheng, R.C.; Li, Y.; Dai, C.C.; Gao, B.Y.; Hu, X.Q.; Wang, C.Y. Depositional features of debris flow of submarine fan in Zhujiang Formation, Baiyun Sag. *J. Jilin Univ.* **2012**, *42*, 1581–1589.
21. Shanmugam, G. *New Perspectives on Deep-Water Sandstones: Origin, Recognition, Initiation, and Reservoir Quality*; Elsevier: Amsterdam, The Netherlands, 2003; pp. 154–179.
22. Shanmugam, G. New perspectives on deep-water sandstones: Implications. *Petrol. Explor. Dev.* **2013**, *40*, 316–324. [CrossRef]
23. Wang, Y.; Liu, L.F.; Li, S.T. The Forming Mechanism and Process of Tight Oil Sand Reservoirs: A case study of Chang 8 Oil Layers of the Upper Triassic Yanchang Formation in the Western Jiyuan Area of the Ordos Basin, China. *J. Petro. Sci. Eng.* **2017**, *158*, 29–46. [CrossRef]
24. Feng, C.; Dai, M.; Liu, X.J.; Zhao, M.; Zhang, C. Logging Classification and Recognition of Lacustrine Mixed Sedimentary Reservoirs in First and Second Members of Shahejie Formation in Bohai Sea. *Earth Sci.* **2020**, *45*, 3677–3692.
25. Ding, J.J. Diagenetic Evolution of Chang 7 Tight Sandstone in Zhidan Area and Its Control on Reservoir Physical Properties. Master's Thesis, Xi'an Shiyou University, Xi'an, China, 2025; pp. 1–101.
26. Zhang, J. Enrichment Patterns and Sweet Spot Prediction of the Chang 7 Member Shale Oil in the Fuxian Area, Ordos Basin. Master's Thesis, Xi'an Shiyou University, Xi'an, China, 2025. [CrossRef]

27. Li, Z.H. The Characteristics of Chang 7 Reservoirs and Its Oil Control in Wuqi. Master's Thesis, Xi'an Shiyou University, Xi'an, China, 2025. [CrossRef]
28. Bouma, A.H. *Sedimentology of Some Flysch Deposits*; Elsevier: Amsterdam, The Netherlands, 1962; p. 168.
29. Liu, F.; Zhu, X.M.; Li, Y.; Xu, L.M.; Niu, X.B.; Zhu, S.F.; Liang, X.W.; Xue, M.G.; He, J.C. Sedimentary facies analysis and depositional model of gravity-flow deposits of the Yanchang formation, southwestern Ordos Basin, NW China. *Pet. Exp. Develop.* **2015**, *42*, 633–645. [CrossRef]
30. Zheng, R.C.; Zheng, Z.; Gao, B.Y.; Hu, X.Q.; Wang, C.Y. Sedimentary features of the gravity flows in submarine fan of Zhujiang Formation in Baiyun Sag, Pearl River Mouth Basin. *Litho. Reserv.* **2013**, *25*, 1–8.
31. Shanmugam, G. Deep-marine tidal bottom currents and their reworked sands in modern and ancient submarine canyons. *Mar. Pet. Geol.* **2003**, *20*, 471–491. [CrossRef]
32. Nemec, W. Aspects of sediment movement on steep delta slopes. In *Coarse-Grained Deltas*; Colella, A., Prior, D.B., Eds.; Blackwell Scientific Publications: London, UK, 2009; pp. 29–73.
33. Gao, H.C.; Zheng, R.C.; Wei, Q.L.; Chen, F.L.; Chen, J.; Zhu, D.F.; Liu, Y. Reviews on fluid properties and sedimentary characteristics of debris flows and turbidity currents. *Adv. Earth Sci.* **2012**, *27*, 815–827.
34. Dott, R.H. Dynamics of subaqueous gravity depositional processes. *AAPG Bull.* **1963**, *47*, 104–128. [CrossRef]
35. Shanmugam, G.; Feng, Z.Z.; Liu, M. The seismite problem. *J. Palaeogeogra.* **2017**, *19*, 19–64. [CrossRef]
36. Middleton, G.V.; Hampton, M.A. Subaqueous sediment transport and deposition by sediment gravity flows. In *Marine Sediment Transport and Environmental Management*; Stanley, D.J., Swift, D.J.P., Eds.; John Wiley: New York, NY, USA, 1976; pp. 197–218.
37. Ilstad, T.; Elverhoi, A.; Issler, D.; Marr, J.G. Subaqueous Debris Flow Behaviour and Its Dependence on the Sand/Clay Ratio: A Laboratory Study Using Particle Tracking. *Mar. Geol.* **2004**, *213*, 415–438. [CrossRef]
38. Lü, Q.Q.; Wang, L.; Luo, S.S.; Liu, J.H.; You, Y.; Yan, H.G.; Pu, Y.X.; Sun, X.H.; Zhang, L. Preliminary Study of the Dynamic Mechanism of Lacustrine Fine-Grained Turbidity Deposits Based on a Flume Sedimentary Simulation. *Acta Sediment. Sin.* **2025**, *43*, 769–781.

Disclaimer/Publisher's Note: The statements, opinions and data contained in all publications are solely those of the individual author(s) and contributor(s) and not of MDPI and/or the editor(s). MDPI and/or the editor(s) disclaim responsibility for any injury to people or property resulting from any ideas, methods, instructions or products referred to in the content.